Solid State Electrochemically Generated Luminescence Based on Serial Frozen Concentration Gradients of $Ru^{III/II}$ and $Ru^{II/I}$ Couples in a Molten Ruthenium 2,2′-Bipyridine Complex

Karolyn M. Maness,† Hitoshi Masui, R. Mark Wightman, and Royce W. Murray*

Contribution from the Kenan Laboratories of Chemistry, University of North Carolina, Chapel Hill, North Carolina 27599-3290

Received October 23, 1996[⊗]

Abstract: The attachment of two polyethylene glycol tails ($n = 7$, MW = 350) to ruthenium tris(bipyridine) via ester links on the 4,4′-positions of one of the bipyridine ligands yields a highly viscous ($\eta \approx 10^7$ cP) molten salt (abbreviated $[Ru(bpy)_2(bpy(CO_2MePEG350)_2)](ClO_4)_2$) that glasses at *ca.* −5 °C. At room temperature, the ionic conductivity of the melt is sufficiently high that application of 2.4 V across the fingers of a Pt interdigitated electrode array (IDA) coated with the melt leads to the electrolytic development of serial concentration gradient microstructures of $Ru^{III/II}$ and $Ru^{II/I}$ states. At the intersection of the two concentration gradients, in the interior of the coating, reaction between the Ru^{III} and Ru^{I} states leads to ECL emission with an efficiency of 0.2% photons/electron. Cooling a concentration gradient-containing film to −20 °C under voltage bias, so as to preserve the gradient microstructure, yields a film that has an emission efficiency of 0.1%, a current and light emission response that rapidly changes with the applied voltage bias, and a diode-like current−voltage profile with a *ca.* 100 rectification ratio.

In a previous communication,[1] we described a new approach to eliciting electrogenerated chemiluminescence (ECL) from dry, solid state films of the electropolymerized redox polymer poly-$[[Ru(vbpy)_3](PF_6)_2]$ (vbpy = 4-vinyl-4′-methyl-2,2′-bipyridine), in which there were serial, frozen concentration gradients of $Ru^{III/II}$ and $Ru^{II/I}$ oxidation states. Electronic conductivity in these and other dry mixed valent redox polymer films[2] occurs by electron self-exchange (hopping) reactions between their electronically localized, physically immobile redox sites. The poly$[[Ru(vbpy)_3](PF_6)_2]$ films exhibit ECL emission from excited state sites formed by the reaction between the Ru^{III} and Ru^{I} states at the interface of the two concentration gradients. We demonstrated[1] that films containing the gradient microstructures, when cooled and dried to limit counterion mobility, are still able to produce ECL emissions, and although the chemical mechanism of ECL emission is unchanged, the current and light emission *response* of the cool, dry films differ in many ways from those typical of ECL from other polymer films.[3]

Chart 1

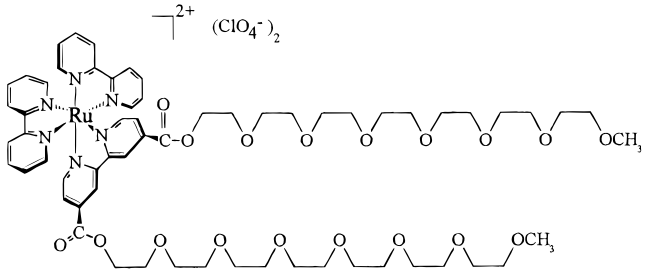

Namely, the rise times for the onset of current flow and light emission upon application of a voltage bias are short,[2b,4] currents do not exhibit limiting plateaus, and currents and light emission exhibit diode-like properties, being greatly favored in the voltage bias direction originally used to form the concentration gradients.

In this work, this concept[1] of solid state ECL is extended using the *monomeric* ruthenium bipyridine complex[5] shown in Chart 1. This "two-tail" version of the famous $[Ru(bpy)_3]^{2+}$ complex, which we abbreviate $[Ru(bpy)_2(bpy(CO_2MePEG350)_2)](ClO_4)_2$, is a viscous ($\eta \approx 10^7$ cP), room temperature molten salt, which has an apparent, broad glassing transition at *ca.* −5 °C.[5] This material, having a 0.94 M concentration of Ru complex sites, is one of a family[5,6] of variously polyether-tailed cobalt, iron, and ruthenium bipyridine complexes, which are

* To whom correspondence should be addressed.
† Present address: Upjohn Co., Kalamazoo, MI 49008.
⊗ Abstract published in *Advance ACS Abstracts,* April 1, 1997.

(1) Maness, K. M.; Terrill, R. H.; Meyer, T. J.; Murray, R. W.; Wightman, R. M. *J. Am. Chem. Soc.* **1996**, *118*, 10609.
(2) (a) Jernigan, J. C.; Murray, R. W. *J. Am. Chem. Soc.* **1987**, *109*, 1738. (b) Jernigan, J. C.; Surridge, N.; Zvanut, M. E.; Silver, M.; Murray, R. W. *J. Phys. Chem.* **1989**, *93*, 4620. (c) Dalton, E. F.; Surridge, N. A.; Jernigan, J. C.; Wilbourn, K. O.; Facci, J. S.; Murray, R. W. *Chem. Phys.* **1990**, *141*, 143. (d) Surridge, N. A.; Zvanut, M. E.; Keene, F. R.; Sosnoff, C. S.; Silver, M.; Murray, R. W. *J. Phys. Chem.* **1992**, *96*, 962. (e) Sullivan, M. G.; Murray, R. W. *J. Phys. Chem.* **1994**, *98*, 4343. (f) Terrill, R. H.; Hatazawa, T.; Murray, R. W. *J. Phys. Chem.* **1995**, *98*, 5127. (g) Terrill, R. H.; Hatazawa, T.; Murray, R. W. *J. Phys. Chem.* **1995**, *99*, 16676. (h) Rosseinsky, D. R.; Monk, P. M. S. *J. Chem. Soc., Faraday Trans.* **1994**, *90*, 1127. (i) Cannon, R. D.; Jayasooriya, U. A.; Anson, C. E.; White, R. P.; Tasset, F.; Ballou, R.; Rosseinsky, D. R. *J. Chem. Soc., Chem. Commun.* **1992**, *19*, 1445. (j) Hursthouse, M. B.; Quillin, K. C.; Rosseinsky, D. R. *J. Chem. Soc., Faraday Trans.* **1992**, *88*, 3071. (k) Rosseinsky, D. R.; Tonge, J. S. *J. Chem. Soc., Faraday Trans.* **1987**, *83*, 245. (l) Rosseinsky, D. R.; Tonge, J. S.; Bertheolot, J.; Cassidy, J. F. *J. Chem. Soc., Faraday Trans* **1987**, *83*, 231. (m) Facci, J. S.; Abkowitz, M.; Linburg, W.; Knier, F. *J. Phys. Chem.* **1992**, *95*, 7908. (n) Facci, J. S.; Abkowitz, M. A.; Limburg, W. W.; Renfer, D. S.; Yanus, J. F. *Mol. Cryst. Liq. Cryst.* **1991**, *194*, 55. (o) Abkowitz, M. A.; Facci, J. S.; Limburg, W. W.; Yanus, J. F. *Phys. Rev. B: Condens. Matter* **1992**, *46*, 6705.
(3) (a) Rubinstein, I.; Bard, A. J. *J. Am. Chem. Soc.* **1981**, *103*, 5007. (b) Fan, F.-R. F.; Mau, A.; Bard, A. J. *Chem. Phys. Lett.* **1985**, *116*, 400. (c) Abruna, H. D. *J. Electrochem. Soc.* **1985**, *132*, 842. (d) Zhang, X.; Bard, A. J. *J. Phys. Chem.* **1988**, *92*, 5566. (e) Miller, C. J.; McCord, P. *Langmuir* **1991**, *7*, 2781. (f) Obeng, Y. S.; Bard, A. J. *Langmuir* **1991**, *7*, 195. (g) Xu, X.; Bard, A. J. *Langmuir* **1994**, *10*, 2409. (h) Richter, M. M.; Fan, F. F.; Klavetter, F.; Heeger, A. J.; Bard, A. J. *Chem. Phys. Lett.* **1994**, *226*, 115. (i) Pei, Q.; Yu, G.; Zhang, C.; Yang, Y.; Heeger, A. J. *Science* **1995**, *269*, 1086. (j) Pei, Q.; Yang, Y.; Gang, Y.; Chi, Z.; Heeger, A. J. *J. Am. Chem. Soc.* **1996**, *118*, 3922.
(4) When the ionic population of a mixed valent redox polymer is immobilized, the electron hopping reaction rate can be characterized in terms of the applied electric field and depends exponentially on the applied voltage bias.
(5) Masui, H.; Murray, R. W. Manuscript in preparation.

S0002-7863(96)03675-X CCC: $14.00

all room temperature molten salts, characterized by very large room temperature viscosities, very small physical self-diffusion coefficients (D_{PHYS} near 10^{-13} cm^2/s for [Co(bpy(CO$_2$MePEG350)$_2$)$_3$](ClO$_4$)$_2$), and generally large ($Co^{II/I}$, $Fe^{III/II}$, $Ru^{III/II} > 10^5$ M^{-1} s^{-1}) electron self-exchange rate constants. At room temperature, the ionic conductivity of [Ru(bpy)$_2$(bpy(CO$_2$MePEG350)$_2$)](ClO$_4$)$_2$ is 1×10^{-8} Ω^{-1} cm^{-1} whereas at the temperature of its apparent glass transition (−5 °C) it has fallen to *ca.* 1×10^{-11} Ω^{-1} cm^{-1}. An objective of this work is to exploit this difference in ionic mobility to form serial concentration gradients in films of [Ru(bpy)$_2$(bpy(CO$_2$MePEG350)$_2$)](ClO$_4$)$_2$ at room temperature and then to stably "freeze" them in place by quenching ionic transport at lowered temperatures.

The reaction leading to ECL emission from ruthenium bipyridine complexes is well known.[7] The one-electron oxidation (abbreviated Ru^{III}) and reduction (abbreviated Ru^{I}) products of solution phase $[Ru(bpy)_3]^{2+}$ (abbreviated Ru^{II}) or of its polymer phase analogs[8] react to give the excited state complex $[Ru(bpy)_3]^{2+*}$ (abbreviated Ru^{II*}), which luminesces, viz.,

$$Ru^{III} + Ru^{I} \rightarrow Ru^{II*} + Ru^{II} \rightarrow 2Ru^{II} + h\nu \qquad (1)$$

ECL emission has been observed in poly[[Ru(vbpy)$_3$](PF$_6$)$_2$] films using interdigitated array (IDA) electrodes,[1] and in solutions of $[Ru(bpy)_3]^{2+}$ using adjacent band electrodes[9] and IDA electrodes.[10]

We show here that films of the *undiluted* molten salt[5] [Ru(bpy)$_2$(bpy(CO$_2$MePEG350)$_2$)](ClO$_4$)$_2$ on an IDA electrode also exhibit ECL emission under appropriate voltage bias. At room temperature, the emission develops slowly with time since it requires electrolytic conversion of the Ru^{II} complexes to Ru^{III} and Ru^{I} complexes at the anode and cathode, respectively, and the transport of these states to an intersecting emission region. These processes depend on the rate of rearrangement of the counterion population in the film that is necessary to satisfy electroneutrality. As the film develops mixtures of Ru^{III}/Ru^{II} and Ru^{II}/Ru^{I} at the positive and negative electrodes, respectively, electron hopping between adjacent electron donors and acceptors brings the Ru^{III} and Ru^{I} states together within the interior of the film and light emission commences. Eventually, the concentration profiles of the Ru^{III}, Ru^{II}, and Ru^{I} species reach a steady state, producing the microstructured arrangement of oxidation states shown in Figure 1. At steady state, the electron hopping current is no longer accompanied by a net movement of counterions. Figure 1 is based on calculations using the electron transport parameters of the Ru complex melt (*vide infra*); similar calculations have been described previously in the context of "ion-budgeted", steady state systems.[11]

The concentration profiles in Figure 1 are generated at room temperature, where the ionic conductivity suffices for the electrolytic processes to readily proceed. As is true in fluid solution experiments, the ionic conductivity of the melt is, at room temperature, sufficient to allow relaxation of the concentration gradients if the voltage bias is removed, and to reverse them if the bias is reversed. However, when the film temperature is lowered so as to depress the ionic mobility, the concentration gradients become "frozen" in place over a time scale long enough so that electron hopping is the sole mode of charge transport during the experiment. The properties of the film are then quite different, as we will show: the film exhibits diode-like behavior with respect to current and light emission, and the current and light emission respond rapidly to changes in applied voltage bias. These characteristics were seen[1] for cooled films of poly[[Ru(vbpy)$_3$](PF$_6$)$_2$], but are improved in the present [Ru(bpy)$_2$(bpy(CO$_2$MePEG350)$_2$)](ClO$_4$)$_2$ material with respect to rectification ratio and ECL quantum efficiencies. These improvements have their origin in the better quenching of ionic transport and (possibly) in the reduced rates of nonradiative excited state relaxation.

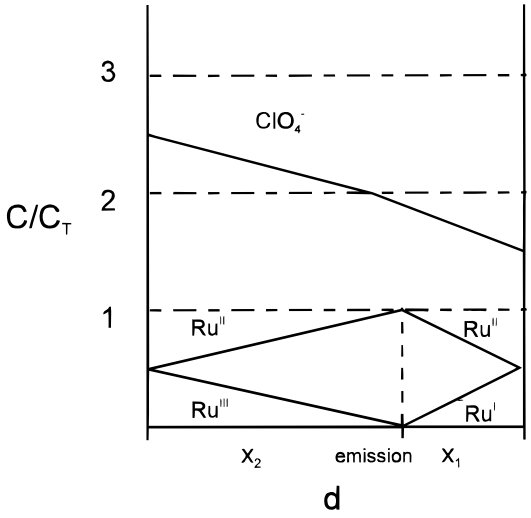

Figure 1. A schematic of the steady state concentration gradients of redox products formed by applying 2.4 V to a [Ru(bpy)$_2$(bpy(CO$_2$MePEG350)$_2$)](ClO$_4$)$_2$ (concentration C_T) coated IDA. The applied voltage is equal to the difference in formal potentials (for reasons described before[1]) of the $Ru^{III/II}$ and $Ru^{II/I}$ redox processes of the film. The fingers of the IDA are approximated as parallel plates, and the film is sandwiched between them. The left and right fingers represent the anode and cathode, respectively.

Experimental Section

Chemicals. Synthesis of [Ru(bpy)$_2$(bpy(CO$_2$MePEG350)$_2$)](ClO$_4$)$_2$.[5] A propylene carbonate solution containing 0.16 g of [Ru(bpy)$_2$Cl$_2$], 0.15 g of AgClO$_4$·H$_2$O, and 0.3 g of bpy(CO$_2$MePEG350) ligand (see Chart 1; the methyl-terminated poly(ethylene glycol) "tails" have an average MW = 350 which corresponds to seven repeat units) was stirred for 15 h at 85 °C. The solvent was removed at 85 °C under vacuum, and 5 mL of H$_2$O was added, causing AgCl to precipitate. The precipitate was removed by centrifugation, and the aqueous solution was extracted with benzene to remove unreacted ligand. The H$_2$O was removed via rotary evaporation, and the final pure red brown oil was dried under vacuum at 70 °C.

9,10-Diphenylanthracene (DPA) and tetra-*n*-butylammonium hexafluorophosphate (Bu$_4$NPF$_6$) were recrystallized twice from absolute and 95% ethanol, respectively, and dried for several hours under reduced pressure at 60 °C. Acetonitrile and toluene (UV grade, Burdick and Jackson) employed for solution ECL were sparged with N$_2$ and passed through an activated alumina column. Solutions were prepared in an inert atmosphere glovebox. All chemicals, except as noted, were reagent grade or better (Aldrich).

IDA Electrodes and Cell. The interdigitated array (IDA) electrodes consisted of 100 platinum fingers (n_F), which were 3 μm wide (w), 2 mm long (l), and 0.15 μm thick (h), and were separated by 2 μm gaps (d). The electrodes were microlithographically patterned on Si/SiO$_2$ substrates, with a chromium underlayer, and an insulating Si$_3$N$_4$ overlayer surrounding the electrode pattern. These devices, generously

(6) (a) Long, J. W.; Velazquez, C. S.; Murray, R. W. *J. Phys. Chem.* **1995**, *100*, 5492. (b) Williams, M.-B.; Masui, H.; Long, J. W.; Malik, J.; Murray, R. W. *J. Am. Chem. Soc.* **1997**, *119*, 1997.

(7) (a) Faulkner, L. R.; Bard, A. J. In *Electroanalytical Chemistry*; Bard, A. J., Ed.; Marcel Dekker: New York, 1977; Vol. 10, pp 1−95. (b) Wallace, W. L.; Bard, A. J. *J. Phys. Chem.* **1979**, *83*, 1350.

(8) Abruna, H. D.; Bard, A. J. *J. Am. Chem. Soc.* **1982**, *104*, 2641.

(9) Bartelt, J. E.; Drew, S. M.; Wightman, R. M. *J. Electrochem. Soc.* **1992**, *138*, 70.

(10) Chidsey, C. E.; Feldman, B. J.; Lundgren, C.; Murray, R. W. *Anal. Chem.* **1986**, *58*, 601.

(11) Jernigan, J. C.; Chidsey, C. E. D.; Murray, R. W. *J. Am. Chem. Soc.* **1985**, *107*, 2824.

donated by Drs. M. Morita and O. Niwa of Nippon Telephone and Telegraph, were cleaned by wiping with a 2-propanol-soaked swab, rinsing with 2-propanol, and drying in a N_2 stream. The IDAs were secured to a Teflon holder, allowing reproducible placement in front of a photomultiplier tube. The holder was mounted in a cell[1] which provided N_2 bathing gas, vacuum evacuation, or addition of a solution of the Ru complex, and contained a Pt mesh auxiliary electrode and Ag wire quasi-reference electrode.

Film Preparation, Characterization, and Concentration Gradient Formation. $[Ru(bpy)_2(bpy(CO_2MePEG350)_2)](ClO_4)_2$ films were drop-cast onto the IDA fingers from a fairly concentrated methanol−water solution, removing the solvent by evaporation. The roughly circular films completely covered the IDA fingers, and appeared to have uniform thickness except for the thicker edges as is typical for drop-cast films. The average film thickness was determined by dissolving the film in a known volume of acetonitrile and spectrophotometrically measuring (480 nm, $\epsilon = 1.46 \times 10^4$)[5,12] the $[Ru(bpy)_2(bpy(CO_2MePEG350)_2)](ClO_4)_2$ concentration.

The film-coated IDAs were placed in the ECL cell, which was evacuated for 5 min and then back-filled with dry N_2. Steady state serial concentration gradients of $Ru^{III/II}$ and $Ru^{II/I}$ were generated in the dry film by application of a 2.4 V bias across the IDA finger sets at room temperature until steady state currents were attained. Under bias, the films were cooled with a N_2 stream whose temperature was maintained by being chilled by liquid N_2 and then heated to a controlled temperature using the output of an Omega CN76000 temperature controller. The controlling thermocouple (T-type) was located adjacent to the IDA electrode. The interfinger voltage bias (ΔE) was maintained at all times to preserve the electrolytically generated concentration gradients while the temperature was lowered through the melt glassing transition to quench macroscopic ion transport. Any changes in the gradients during cooling (such as might arise from temperature dependencies of formal potentials) are in the face of falling ionic conductivities probably incompletely consummated. Such effects are of minor consequence to the present discussion and are neglected.

Current−Voltage and Electrogenerated Chemiluminescence Measurements. Current−voltage responses of cooled, concentration gradient-containing films were examined with voltage step and sweep biases applied across the IDA finger sets. The voltage was controlled by an IBM PC compatible microcomputer, equipped with a Datel 412 analog IO board, running a locally written program. For biases greater than ±5 V, a Kepco B0P100-1M bipolar operational power supply (±100 V) amplifier was used to amplify the smaller amplitude voltage waveforms. Film currents were monitored with either a Pine Model AFCP1 or an Ensman Instruments EI400 bipotentiostat.

ECL emission was measured with a Hamamatsu R928 photomultiplier tube (PMT) operated at −600 V. The solid aluminum Faraday cage surrounding the ECL cell was lined with black felt to block ambient light. The PMT current was measured with a Stanford Research Systems Model SR570 low-noise current preamplifier and recorded on a Nicolet 310 digital oscilloscope, strip chart recorder, or the Datel 412 IO board and microcomputer.

The ECL efficiency ϕ_{ECL} is defined as the number of photons emitted per electron. The PMT current scale was calibrated with the emission from a 1 mM diphenylanthracene (DPA) solution in 0.1 M Bu_4NPF_6/50:50 (v/v) CH_3CN/toluene, which has a ϕ_{ECL} of 0.064 ± 0.005.[13] The intensity measurements were corrected for differences in PMT sensitivity at the wavelengths of maximum emission using the manufacturer's specifications.

Luminescence measurements of $[Ru(bpy)_2(bpy(CO_2MePEG350)_2)](ClO_4)_2$ in acetonitrile solutions and as neat films dried and cast from methanol solutions onto glass slides were obtained using a Spex Fluorolog F212 emission spectrometer. The data were corrected for the wavelength dependent sensitivity of the instrument, and quantum yields were referenced to a dilute $[Ru(bpy)_3](ClO_4)_2$ solution in acetonitrile.[7b]

Conductivity Measurements. Electronic (dc) conductivities of $[Ru(bpy)_2(bpy(CO_2MePEG350)_2)](ClO_4)_2$ films on IDA electrodes were measured in the ECL cell to facilitate direct comparisons with ECL and diode results. They were determined for films with preformed, serial concentration gradients of $Ru^{III/II}$ and $Ru^{II/I}$ that had been generated with a 2.4 V bias at room temperature. Currents measured at the 2.4 V bias were converted to conductivities using the geometrical cell constant, d/A, of the IDA, where d is interelectrode gap width and A is the area of the approximate parallel plate sandwich ($A = (n_F - 1)lh$).

The ionic conductivities of the films (in the Ru^{II} oxidation state) were measured under vacuum on a home-built, thermally controlled stage.[14] Between 60 and 0 °C, ac impedance spectroscopy was used (Schlumberger Model 1287 electrochemical interface and 1260 impedance/gain phase analyzer; 20−100 mV amplitude), and at lower temperatures, fast (1 V/s) linear sweep, current-voltage plots were analyzed. The cell constant of the IDA used for these measurements was determined to be 0.0447 cm^{-1} using a polymer electrolyte of measured ionic conductivity (0.25 M LiCl in poly(propylene glycol)).

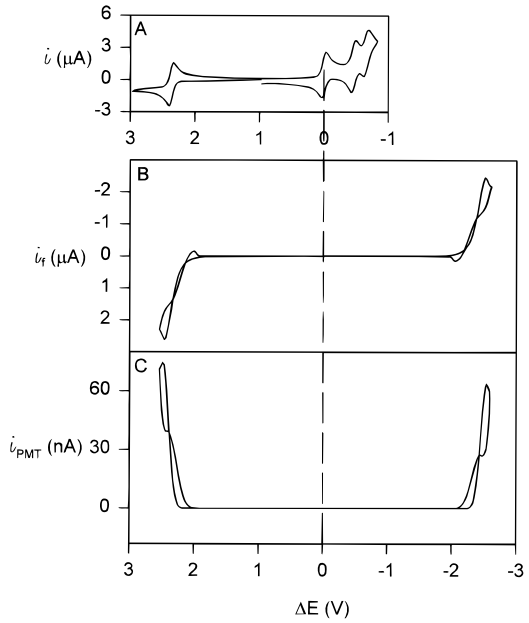

Figure 2. Electrochemical properties of $[Ru(bpy)_2(bpy(CO_2MePEG350)_2)](ClO_4)_2$ in solution and as neat liquid films. Panel A: Cyclic voltammogram (200 mV/s) of 2 mM $[Ru(bpy)_2(bpy(CO_2MePEG350)_2)](ClO_4)_2$ in acetonitrile containing 0.1 M Bu_4NPF_6 at a 0.25 mm radius Pt disk electrode. Panels B and C: Current and light emission observed at 50 °C for a neat 1.4 μm thick $[Ru(bpy)_2(bpy(CO_2MePEG350)_2)](ClO_4)_2$ film deposited on a Pt IDA in response to 5 mV/s voltage sweep from 0 to +2.6 to −2.6 to 0 V.

Results

Solution Properties of $[Ru(bpy)_2(bpy(CO_2MePEG350)_2)](ClO_4)_2$. A cyclic voltammogram of 2 mM $[Ru(bpy)_2(bpy(CO_2MePEG350)_2)](ClO_4)_2$ in acetonitrile containing 0.1 M (Bu_4NPF_6) is shown in Figure 2A. From this, the formal potentials were determined to be 1.37 V vs SCE for the $Ru^{III/II}$ couple and −1.03 V vs SCE for the $Ru^{II/I}$ couple, corresponding to a formal potential difference of $\Delta E° = 2.40$ V.

The wavelength of maximum luminescence for $[Ru(bpy)_2(bpy(CO_2MePEG350)_2)](ClO_4)_2$ in acetonitrile is 690 nm using 480 nm excitation; the luminescence quantum yield, ϕ_E, was determined to be 0.057. The steady state ECL emission of $[Ru(bpy)_2(bpy(CO_2MePEG350)_2)](ClO_4)_2$ in acetonitrile, contacting an IDA with an applied voltage bias of 2.4 V, has a ϕ_{ECL} of 0.0048. By comparison, $[Ru(bpy)_3]^{2+}$ has a ϕ_E of 0.075 and a ϕ_{ECL} of 0.05 at 25 °C.[7b] Although both compounds have similar ϕ_E values, the $[Ru(bpy)_2(bpy(CO_2MePEG350)_2)]^{2+}$

(12) Elliott, C. M.; Hershenhart, E. J. *J. Am. Chem. Soc.* **1982**, *104*, 7519.
(13) Maness, K. M.; Bartelt, J. E.; Wightman, R. M. *J. Phys. Chem.* **1994**, *98*, 3993.
(14) Hatazawa, T.; Terrill, R. H.; Murray, R. W. *Anal. Chem.* **1996**, *68*, 597.

complex has a much smaller ϕ_{ECL} value, which indicates that the emissive excited state of the tailed species is produced less efficiently in the ion annihilation reaction. The reasons for this difference have not been explored; we note the lower coordination symmetry and differences in formal potentials[5] of the ring reductions as possible factors.

ECL Production in Room Temperature and Warmed Films. Films of neat $[Ru(bpy)_2(bpy(CO_2MePEG350)_2)](ClO_4)_2$, when excited at 480 nm, have an emission maximum at 697 nm, close to that of their solutions. Slowly scanning the voltage bias applied across the fingers of a $[Ru(bpy)_2(bpy(CO_2MePEG350)_2)](ClO_4)_2$-coated IDA at 50 °C results in current−voltage curves as shown in Figure 2B. The currents that rise at voltages larger than ±2 V reflect the electrolysis of the Ru^{II} complex into its Ru^{III} and Ru^{I} states. The half-wave potential of the rise is *ca.* 2.4 V, which is consistent with the $Ru^{III/II}$ and $Ru^{II/I}$ formal potentials observed in acetonitrile solution.[15] The very appearance of the electrolytic currents and the fact that the current−voltage curve is symmetrical about $\Delta E = 0$ mean that ionic transport in the warm melt is facile on the voltage sweep time scale. Thus, in the neat 50 °C $[Ru(bpy)_2(bpy(CO_2MePEG350)_2)](ClO_4)_2$ melt, the serial concentration gradients established at steady state (long time) by a 2.4 V bias (i.e., Figure 1) can be fairly quickly reversed by electrolysis at a −2.4 V bias. The presence of peaks and hysteresis in the current−voltage curves in Figure 2B means simply that the potential sweep rates employed were not small enough to completely establish the steady state concentration gradients of Figure 1 (plus perhaps a minor iR potential loss). The current flow in Figure 2B is accompanied by light emission from the film (Figure 2C) as expected for the ECL reaction. Emission occurs in both directions of voltage bias, again consistent with a facile reversal of the concentration gradients with the polarity of the voltage bias.

Figure 3 (top) shows the use of potential steps to initiate current flow (—) and ECL emission (- - -) from a neat $[Ru(bpy)_2(bpy(CO_2MePEG350)_2)](ClO_4)_2$ film on an IDA at room temperature. Given the agreement between the half-wave potentials in Figure 2B and the difference in $Ru^{III/II}$ and $Ru^{II/I}$ formal potentials in Figure 2A, the 2.4 V bias drives the electrode/melt interfacial concentrations to values such that $C_{Ru^{II}} \approx C_{Ru^{III}}$ and $C_{Ru^{II}} \approx C_{Ru^{I}}$ at the positively and negatively biased IDA fingers, respectively (i.e., Figure 1). The potential step produces a small transient current spike followed by a slow rise toward a steady state plateau. The ECL light emission also rises toward a steady state plateau, but as seen before[1] and as is discussed (*vide infra*), the onset is somewhat delayed from the time of voltage bias application. Application of a 2.4 V bias of opposite sign (not shown) gives the same current and light emission vs time profile but with the current of opposite polarity.

The efficiency of the room temperature ECL emission from $[Ru(bpy)_2(bpy(CO_2MePEG350)_2)](ClO_4)_2$ films, as shown in Figure 3, was 0.0019 ± 0.0003 ($n = 7$). This ECL efficiency is within a factor of 2 of that observed in dilute acetonitrile solutions. Additionally, the ECL efficiency is both more reproducible and much larger than that of electropolymerized films of poly[$[Ru(vbpy)_3](PF_6)_2$] studied in analogous potential step experiments ($\phi_{ECL} = 0.0003$).[1]

(15) (a) To the extent that the difference in the formal potentials of the $Ru^{III/II}$ and $Ru^{II/I}$ couples determined in acetonitrile (Figure 2A) are not exactly the same as in the neat material (Figure 2B), the concentration gradients formed in the neat film upon application of 2.4 V would not adhere exactly to those depicted in Figure 1. However, prior evidence[15b] indicates that redox couple formal potentials do not differ significantly between polyether and acetonitrile solvents. (b) Reed, R. A.; Geng, L.; Murray, R. W. *J. Electroanal. Chem.* **1986**, *208*, 185.

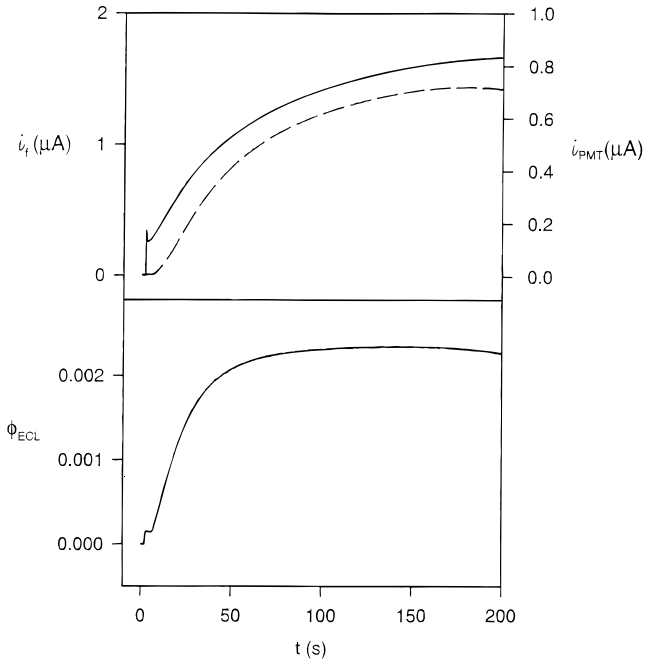

Figure 3. Room temperature (23.4 °C) time dependence of current (—), light emission (- - -), and ECL efficiency of a *ca.* 2 μm thick $[Ru(bpy)_2(bpy(CO_2MePEG350)_2)](ClO_4)_2$ film coated on a Pt IDA, upon application of 2.4 V.

Figure 1 shows the theoretical position of the emission region (Figure 1) near the center of the interfinger gap region. The position arises from the joint constraints of $C_{Ru^{II}} \approx C_{Ru^{III}}$ and $C_{Ru^{II}} \approx C_{Ru^{I}}$ at the positively and negatively biased IDA fingers, respectively (*vide supra*), and from the fact that there is no net movement of ions into or out of the $[Ru(bpy)_2(bpy(CO_2MePEG350)_2)](ClO_4)_2$ film (ion-budgeted voltammetry).[11]

Diffusion in Room Temperature Films. Values of the apparent diffusion coefficients (D_{APP}) operant for each couple were independently determined[5] by digital simulation and matching (including accounting for iR effects) of slow scan cyclic voltammograms at a 5 μm radius Pt disk electrode in neat $[Ru(bpy)_2(bpy(CO_2MePEG350)_2)](ClO_4)_2$ at 23.4 °C. The results are $D_{APP(III/II)} = 1.1 \times 10^{-9}$ cm^2/s and $D_{APP(II/I)} = 5.0 \times 10^{-10}$ cm^2/s for the $Ru^{III/II}$ and $Ru^{II/I}$ couples, respectively. These apparent diffusion coefficients are thought[16] to mainly reflect the rate of electron hopping reactions in the respective mixed valent diffusion layers. The fact that they differ for the $Ru^{III/II}$ and $Ru^{II/I}$ couples shows that the rate of electron self-exchange reactions is slightly faster for the $Ru^{III/II}$ couple.

The apparent diffusion coefficients are important in understanding why the initiation of light emission in Figure 3 (top) lags behind the current flow. The time delays ranged between 4 and 12 s, and reflect the time required for the encounter of electrolytically generated Ru^{III} and Ru^{I} states within the interelectrode gap. According to the approximate relationship $t = (x_2)^2/(2D_{APP(II/I)})$ where $x_2 = 1$ μm, the anticipated delay is 10 s which is consistent with the experimental observations.

Film Conductivity. The molten salt $[Ru(bpy)_2(bpy(CO_2MePEG350)_2)](ClO_4)_2$ is either a purely ionic or a mixed ionic/electronic conductor, depending on its oxidation state. The Ru^{II} form is only ionically conductive (not being mixed valent). The

(16) (a) The evidence that the value of D_{APP} is dominated by electron hopping and not physical diffusion of the Ru complexes is discussed elsewhere.[5] The analysis is based on observations that a similarly polyether-tailed cobalt bipyridine complex exhibits[16b] a physical diffusion coefficient of 3×10^{-13} cm^2/s, which is much smaller than the higher apparent diffusion coefficients measured in the current material. (b) Velazquez, C. S.; Hutchison, J. E.; Murray, R. W. *J. Am. Chem. Soc.* **1993**, *115*, 7896.

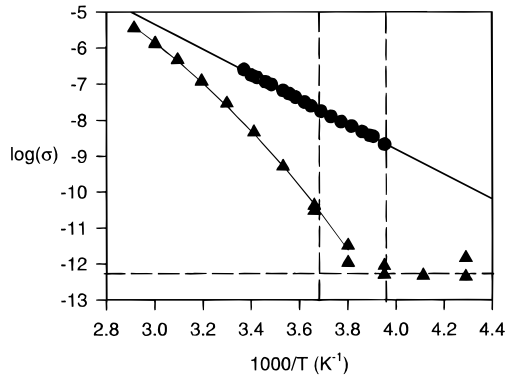

Figure 4. Activation plots of ionic and electronic conductivity of films of $[Ru(bpy)_2(bpy(CO_2MePEG350)_2)](ClO_4)_2$ on IDAs with 2 μm gaps: (▲) ionic conductivity of a film in the Ru^{II} state, deposited on an IDA with 10 μm wide fingers ($\Delta E = 0$); (●) electronic conductivity of a film deposited on an IDA with 3 μm wide fingers and biased at $\Delta E = 2.4$ V. The vertical dashed lines represent the spread of temperatures over which the broad glassing transition (centered at −5 °C) of the melt occurs.

estimated transference numbers for the Ru^{II} melt indicate[5] that the perchlorate counterion is the dominant ionic charge carrier. The room temperature ionic conductivity of the Ru^{II} melt is 1×10^{-8} Ω^{-1} cm^{-1}; Figure 4 (▲) presents conductivity results at varied temperatures as an activation plot. The activation plot is nonlinear as is typical for a physical transport process strongly coupled to segmental motions of polymeric or oligomeric chains. The nonlinearity is seen[6] in other polyether-tailed melts. The limiting ionic conductivity at the lowest temperatures (Figure 4) is almost certainly an artifact caused by the ionic conductivity falling below the leakage conductance between the IDA fingers (a naked IDA in air gave a conductance of 6×10^{-11} Ω^{-1}).

A mixed valent melt ($Ru^{III/II}$ or $Ru^{II/I}$) can be a mixed conductor, i.e., charge transport may involve both ion and electron hopping transport, or it can be solely an electronic conductor with negligibly little ion transport on the experimental time scale. Relationships between experimental conductivities and electron transfer rate constants have been described for concentration gradient-free mixed valent films[2a−f] and for those that contain a single pair of gradients.[2g] A $[Ru(bpy)_2(bpy(CO_2MePEG350)_2)](ClO_4)_2$ film biased at $\Delta E = 2.4$ V contains two sets of concentration gradients (Figure 1); the electronic (dc) conductivity of such a mixed valent film is shown in Figure 4 (●) as an activation plot. The conductivity of the gradient-containing film at steady state should be primarily determined by the rate of electron hopping, since at steady state, net ionic transport has ceased. The activation plot for electronic conductivity (Figure 4, ●) is linear, indicating that coupling between the electron hopping and the polyether tail motions is weaker than in ion transport. The 2.4 V biased films in Figure 4 (●) actively emitted ECL luminescence as the conductivity data were acquired. The electronic conductivity at the lowest temperature (−20 °C) in Figure 4 was 3×10^{-8} Ω^{-1} cm^{-1}; the range of results from other films was 5×10^{-9} to 5×10^{-8} Ω^{-1} cm^{-1} at that temperature.

It is apparent from Figure 4 that, at elevated temperatures, ionic mobilities in the films would be comparable to that of electron hopping, but at lowered temperature, ionic motions are more severely attenuated than are electron hopping reactions. Such differences in the thermal sensitivities of ionic and electronic conductivity in mixed valent redox polymers have been observed before.[2a−f] At the thermal glassing transition[5] (approximately −5 °C) the electronic exceeds the ionic conductivity by 3000-fold. (The actual difference between electron and ion mobilities is even greater than this since the introduction of concentration gradients depresses (several-fold) the observed electronic conductivity as we have described before[2g] in reference to mixed valent viologen films.)

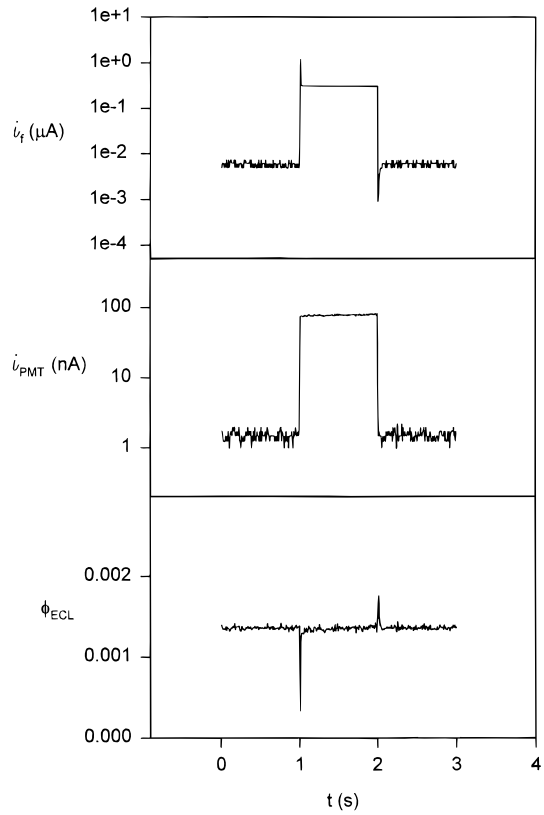

Figure 5. Current (top), light emission (middle), and ECL efficiency (lower) at −20 °C for a *ca.* 1.6 μm thick $[Ru(bpy)_2(bpy(CO_2MePEG350)_2)](ClO_4)_2$ film containing frozen concentration gradients. The applied voltage was stepped from 2.4 to 12.4 (for 1 s) to 2.4 V.

ECL Production in Cooled Concentration Gradient-Containing Films. One may anticipate, from the preceding results, that concentration gradients formed at room temperature should become frozen at lowered temperature, owing to the quenching of ionic mobility. A lack of ionic conductivity should allow the electric field from an impressed voltage bias (of either sign) to be distributed across the entire film (albeit not uniformly[2g]). The rate of generation of Ru^{III} and Ru^{I} states and the intensity of ECL resulting from their recombination then becomes maintained by electric field-driven electron transport. Figure 5 shows the response of a concentration gradient-containing film to a change in bias from $\Delta E = 2.4$ V to $\Delta E = 12.4$ V for 1 s (increased forward bias). Here, forward bias voltages refer to voltages more positive than +2.4 V and reverse bias voltages refer to those more negative than +2.4 V. The fast rise in both current and light emission is characteristic[2a−f] of electric field-driven electron transport through the film; these responses are similar to those observed[1] for poly$[[Ru(vbpy)_3](PF_6)_2]$ films. Both the light and current remain constant during the course of the 10 V forward bias. Although the increases in current and emission intensity that result from the 10 V forward bias are quite large (note the log axis), the ECL *efficiency* remains unchanged during and after the voltage pulse and is thus voltage-independent for this film.[18] The ECL efficiency of the −20 °C film of Figure 5 ($\phi_E = 0.0013$) is nearly the same as that at room temperature ($\phi_E = 0.0019$); thus, the ECL efficiency is also relatively insensitive to temperature.

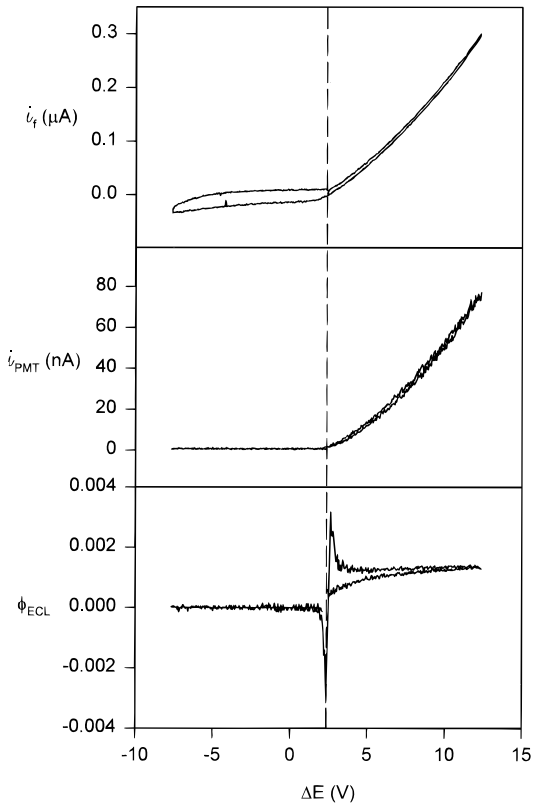

Figure 6. Current (top), light emission (middle), and ECL efficiency (lower) of a $[Ru(bpy)_2(bpy(CO_2MePEG350)_2)](ClO_4)_2$ film containing concentration gradients prepared at room temperature with a $\Delta E = 2.4$ V bias and then frozen at −20 °C. The applied voltage was swept ±10 V at 10 V/s and centered around $\Delta E = 2.4$ V. This figure represents the same film as in Figure 5.

Films cooled to −20 °C without an applied bias (i.e., concentration gradient-free) exhibit neither current flow nor light emission upon application of a voltage bias.

Figure 6 is the key result of this paper. This figure shows the response, at −20 °C, of the film used in Figure 5 to a ±10 V sweep centered around the original $\Delta E = 2.4$ V bias. For forward bias voltages, steep increases are seen in both current and light intensity, analogous to the behavior of electric field-driven electron transport in mixed valent films lacking concentration gradients. The ECL efficiency of this film gradually increases on the sweep toward $\Delta E = 12.4$ V but is relatively constant on the sweep back to $\Delta E = 2.4$ V. Significantly, in the reverse bias scan, no detectable light emission occurs and the currents are small. This diode-like behavior was reproduced in all films examined. Reverse bias conductances were very small, and rectification ratios (ratio of forward to reverse bias conductance) were typically *ca.* 100.

The anticipation that temperatures lower than that of the glass transition (−5 °C) would yield concentration gradient microstructures that are very long-lived even under reverse voltage bias was, however, not realized. Despite the low ionic conductivity of the cooled films, the diode-like behavior could be degraded by prolonged application of a reverse voltage bias as is illustrated in Figure 7. Figure 7A shows a film with diode-like behavior, prepared as in Figure 6, with current and light emission responses resulting from the presence of the frozen concentration gradients. This film was then reverse biased at $\Delta E = -7.6$ V for 10 min. No light and little current flow was observed during this time (not shown). The voltage bias was then briefly returned to 2.4 V, and a ±10 V sweep (like that in Figure 7A) was initiated; Figure 7B shows the result. There is now little increase in current upon forward voltage biasing, and

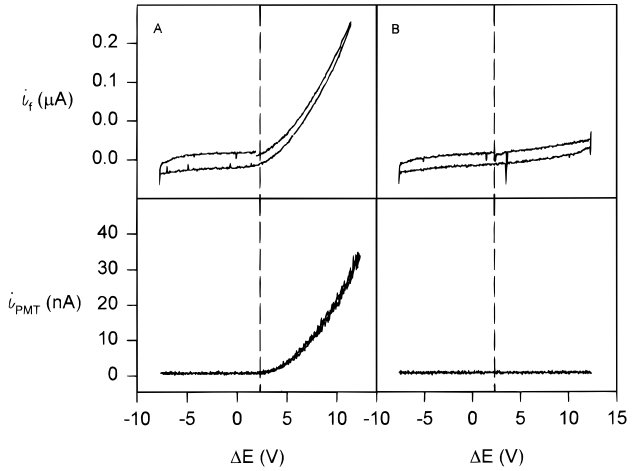

Figure 7. Effect of prolonged reverse bias voltages on the current (top) and light emission (bottom) diode-like properties of a concentration gradient-containing $[Ru(bpy)_2(bpy(CO_2MePEG350)_2)](ClO_4)_2$ film (*ca.* 1.6 μm thick). Panel A: 10 V/s, ±10 V sweep centered at $\Delta E = +2.4$ V. Panel B: ±10 V, 10 V/s voltage sweep centered at $\Delta E = +2.4$ V, following a 10 s long pulse to +12.4 V followed by a 10 min reverse bias at $\Delta E = -7.6$ V.

no light emission at all. Clearly features of the concentration gradient microstructure that are crucial to the diode-like behavior and ECL emission can be degraded by a sufficiently prolonged reverse voltage bias.

Discussion

$[Ru(bpy)_2(bpy(CO_2MePEG350)_2)](ClO_4)_2$ films deposited on IDA electrodes exhibit ECL emission and current flow when serial concentration gradients (Figure 1) are generated by a voltage bias. In a warmed (50 °C) melt, the serial concentration gradients are readily generated under either voltage polarity (Figure 2) because there is sufficient ionic mobility. This situation is identical to that in a fluid solution, and consequently, the ECL-generating currents have limits to their values (the peaks in Figure 2) and the limiting currents and ECL emissions (Figure 3) are only slowly established since the development of serial concentration gradients of $Ru^{III/II}$ and $Ru^{I/II}$ is dictated by the rate of ion transport.

The situation is altered at lowered temperatures, where ionic mobility is reduced. When preformed concentration gradients exist, current only flows when the film is forward biased. Further, no limiting current is reached over a large forward bias range (Figure 5). Current flow in the cooled films is still accompanied by light emission (nearly as efficiently as at higher temperatures), indicating that the ECL reaction continues to occur at the interface of the serial concentration gradients (Figure 1). Now, however, it responds with a fast time constant to changes in voltage bias (Figure 5).

This light-emitting diode-like behavior is analogous to that observed for films of poly$[[Ru(vbpy)_3](PF_6)_2]$ in our previous work.[1] There, the macroscopic mobility of the redox sites was restricted by their incorporation into a cross-linked polymer matrix, and immobility of the PF_6^- counterions was sought by removal of solvent and cooling. These properties are in the present work achieved with a *monomeric* ruthenium complex (Chart 1), in which the physical diffusivity of the ruthenium centers is quite small[5,6] and the ionic conductivity decreases with temperature more rapidly than does electronic conductivity (Figure 4). In both poly$[[Ru(vbpy)_3](PF_6)_2]$ and $[Ru(bpy)_2(bpy(CO_2MePEG350)_2)](ClO_4)_2$, electron hopping between redox sites becomes the dominant conduction mode at low temperature, and large voltage biases can be employed to

accelerate electron transport with short on−off times. The Ru complex melt exhibits improved rectification properties compared to poly[[Ru(vbpy)$_3$](PF$_6$)$_2$] films,[1] currents flowing under reverse bias are much smaller, and a larger reverse bias voltage window is accessible on the time scales of Figure 5. In addition, the ECL efficiencies obtained from [Ru(bpy)$_2$(bpy(CO$_2$MePEG350)$_2$)](ClO$_4$)$_2$ are *ca*. 8 times larger than that obtained from poly[[Ru(vbpy)$_3$](PF$_6$)$_2$] films. Interestingly, the ECL efficiency of the Ru melt in the undiluted state (which contains 0.94 M Ru complex sites) differs little from that in dilute acetonitrile solution, meaning that the operative radiationless decay pathways are concentration independent.

The basis for the diode-like behavior of films containing frozen, serial, concentration gradients of redox sites has been discussed previously.[1] Briefly, application of a forward bias generates Ru^{III} and Ru^{I} states at the positive and negative electrodes, respectively, and transports them by electron hopping to the region where the Ru$^{III/II}$ and Ru$^{II/I}$ concentration gradients intersect. There, they react in a thin depletion region (Figure 1) to form the excited state species, from which light is emitted as in reaction 1. Reverse bias voltages attempt to withdraw Ru^{III} and Ru^{I} states from the gradient intersection, which requires the disproportionation of Ru^{II} sites there, but the voltage dropped over this thin region is insufficient to accomplish that.

The loss of the diode-like property under prolonged reverse bias, as seen in Figure 6, is likely due to electrolytic concentration changes in Ru states, which are allowed by the film's residual ionic conductivity at −20 °C. Although this temperature is below the apparent glass transition temperature observed[5] by differential scanning calorimetry, examples are known[17] of materials that retain ionic conductance below their putative glass transitions, and we infer that the [Ru(bpy)$_2$(bpy(CO$_2$MePEG350)$_2$)](ClO$_4$)$_2$ melt may represent another example of such a material. It is not necessary that the entire concentration gradient microstructure be destroyed for disruption of the film's diode-like behavior. It is likely that the initial and disabling concentration changes occur at the intersection of concentration gradients (Figure 1). The electronic resistivity of gradient-containing films is not spatially uniform;[2g] rather it is largest in regions where electron donor and acceptor concentrations differ greatly (the electron hopping rate is smaller there). The electric field in the film is therefore expected to be largest in the intersection region and provides a greater impetus for ionic motions which then allow electrolytic changes in the Ru state populations. Consequently, there are substantial demands for exceptionally low ionic conductivity in molecular diode experiments utilizing concentration gradient-containing films. In future work, further steps in molecular design will be explored to quench the ionic conductivity of ruthenium bipyridine melts.

The behavior of the Ru complex melts at room and higher temperatures is rather analogous to that reported recently by Pei et al. for conjugated organic polymers.[3i,j] In those experiments, electrolytic generation of oxidized and reduced states at opposing electrodes leads, on a slow time scale, to current flow and light emission from a region within the interelectrode gap. This is the expected behavior for films with relatively immobile redox sites and moderate ionic conductivity. We consider that, under conditions of moderate ionic conductivity, both these examples *are representative of electrochemically generated luminescence*[7] *(ECL) since electrolytic processes lead to the chemical states that emit*.

The Ru complex melt microstructure differs, however, from other polymer light-emitting diodes[19] in that its properties do not need to be explained in terms of a semiconductor model. Rather, the classical view of ECL, as indicated in reaction 1, and the well-known process of electronic hopping between electronically localized sites in mixed valent redox materials[2,3h] (i.e., the Ru complexes) are sufficient to explain the observed results. Further, the electronic conductivity and ECL efficiencies of the concentration gradient-containing Ru complex melts are actually comparable[20] to those reported for the semiconducting poly(phenylenevinylidene) system by Heeger *et al.*,[3j] even though the ruthenium system is based on electron hopping transport. Moreover, the *cooled* melt's emission intensity is capable of being rapidly modulated (Figure 5) with light-emitting diode-like characteristics (Figure 6).

Finally, the present and previous[1] ECL results clearly highlight properties that are required for a practical display device. First, the materials need to have a high degree of electronic conductivity (but low ionic conductivity), which for redox (electron hopping) conductors translates to electron transfer sites with large electron self-exchange reaction rate constants. Second, there must be a balance between the redox site distances; short ones accelerate electron transfer but may increase modes of nonradiative decay. This is suggested by comparing the results from poly[[Ru(vbpy)$_3$](PF$_6$)$_2$] and [Ru(bpy)$_2$(bpy(CO$_2$MePEG350)$_2$)](ClO$_4$)$_2$ films; the former has shorter redox site distances and exhibits a higher electronic conductivity (faster electron diffusion) but a lower ECL efficiency. Third, large voltage gradients are an effective way to increase current flow without damaging light production. In this work, closer electrode spacings were used, as compared to the poly[[Ru(vbpy)$_3$](PF$_6$)$_2$] work, to compensate for the lower electronic conductance of the [Ru(bpy)$_2$(bpy(CO$_2$MePEG350)$_2$)](ClO$_4$)$_2$ films. Finally, the suppression of ionic conductivity in gradient-containing films is important because ionic space charge relaxation prevents application of large sustained voltage gradients across the bulk film, and avoiding electrolysis associated with ionic motions both preserves the gradient microstructure and improves the response times for current and light emission.

Acknowledgment. We thank Dr. T. J. Meyer and co-workers for their help with the luminescence measurements. This research was supported in part by the National Science Foundation and the Department of Energy (R.W.M.).

JA9636754

(17) Angell, C. A. *Solid State Ionics* **1983**, *9* and *10*, 3.

(18) The minor spikes in the Figure 5 ϕ_{ECL} curve are artifacts resulting from the capacitance spikes in the Figure 5 current−time result.

(19) (a) Burroughes, J. H.; Bradley, D. D. C.; Brown, A. R.; Marks, R. N.; Mackay, K.; Friend, R. H.; Burns, P. L.; Holmes, A. B. *Nature* **1990**, *347*, 539. (b) Gustafsson, G.; Cao, Y.; Treacy, G. M.; Klavetter, F.; Colaneri, N.; Heeger, A. J. *Nature* **1992**, *357*, 477. (c) Greenham, N. C.; Moratti S. C.; Bradley, D. C.; Friend, R. H.; Holmes, A. B. *Nature* **1993**, *365*, 628. (d) Berggren, M.; Inganas, O.; Gustafsson, G.; Rasmusson, J.; Andersson, M. R.; Hjertberg, T.; Wennerstrom, O. *Nature* **1994**, *372*, 444.

(20) The Abstract and the data in Figure 3 of ref 3j indicate a room temperature ECL efficiency of 0.003−0.004 electron/photon and an electronic conductivity of $4 \times 10^{-6}\ \Omega^{-1}\ cm^{-1}$; these values are only about 2-fold larger than those reported here.